Reproducing Dust Spectral Backscatter Using Simple Shape Mixtures

Anna Gialitaki [a, b], Alexandra Tsekeri [a], Moritz Haarig [c], Athena Augusta Floutsi [c], Dimitra Kouklaki [a, d], Maria Kezoudi [e], Alkistis Papetta [e], Franco Marenco [e], Konrad Kandler [f], Sudharaj Aryasree [f], Melanie Eknayan [f] and Vassilis Amiridis [a]

[a] IAASARS, National Observatory of Athens, Athens, Greece
[b] School of Physics and Astronomy, Earth Observation Science Group, University of Leicester, UK
[c] Leibniz Institute for Tropospheric Research (TROPOS), Leipzig, Germany
[d] Department of Geology and Geoenvironment, National and Kapodistrian University of Athens
[e] Climate and Atmosphere Research Centre, The Cyprus Institute, Nicosia, Cyprus
[f] Technical University of Darmstadt, Germany
Lead Author e-mail address: togialitaki@noa.gr

Abstract: We explore random mixtures of simplified shapes to reproduce the spectral polarimetric backscattering properties of irregularly shaped desert dust particles. By adopting simplified shapes, this approach mitigates the substantial computational cost associated with the use of realistic particle models, while preserving the spectral backscattering behavior of dust aerosols. Although the primary focus is on lidar applications, sun-photometric and PACE polarimetric observations are used to evaluate the performance of the random mixtures approach across a broader range of scattering angles.

1. Introduction

Through direct and indirect interactions within the Earth's atmosphere, dust particles influence the planetary radiative balance in ways still largely unknown. Current uncertainties arise from multiple factors, including the under-representation of coarse mode dust in atmospheric transport models, as well as uncertainties in dust optical properties related to the uncertainties in complex refractive index (CRI), and the misrepresentation of dust particle shape.

For the calculation of dust optical properties, dust particles are often idealized as smooth, homogeneous spheres in favor of computational efficiency, introducing significant errors, when trying to quantify dust effects on climate [1]. Alternatively, spheroids are utilized from remote sensing retrievals algorithms as the simplest non-spherical shapes that can reproduce the angular behavior of dust aerosols scattering quite well, although deviations are observed in backscattering, which is critical for lidar applications [2]. More complex shapes like irregular hexahedra [3] and even more realistic shapes [4] are available, but they are computationally expensive unless their optical properties are provided in pre-tabulated forms. Nevertheless, accurately reproducing the spectral dependence of dust intensive optical properties remains challenging, even using these shapes. In-situ measurements of aspect ratios are frequently utilized to constrain the particle shapes for optical modelling. However, such datasets can be biased towards smaller aspect ratios [5]. More importantly, when non-realistic, simplified particle shapes like spheroids or ellipsoids, are used to model dust particles it might not be relevant to constrain them with actual measured aspect ratios.

To this end, an alternative approach is pursued in the present study to represent dust particle ensembles, using mixtures of spheroids and irregular hexahedra, and deriving their aspect ratio distributions with no constrain on the shape of the distribution (which can be random as well). Specifically, the weighted mixtures and the aspect ratio distributions are derived to reproduce multi-wavelength lidar observations, of the particle linear depolarization ratio (d_p) and lidar ratio (S_p). These simple-shape mixtures are also used to reproduce multi-angular total and polarized radiances from ground- and satellite-based observations under dusty conditions, serving as an independent consistency check for scattering angles other than backscattering. This approach aims to assess whether our shape model can consistently describe both active and passive remote sensing observations.

2. Calculations of dust optical properties

The scattering properties of spheroidal shapes are derived using the MOPSMAP database [6]. MOPSMAP provides the optical properties of single spherical, spheroidal and irregularly shaped particles in a predefined three-dimensional grid (size-shape-refractive index), for a wide range of size parameters x (up to x~1000 for spheroids) and CRIs.

The scattering properties of irregular hexahedral particles are provided by the TAMUdust2020 database [3]. TAMUdust2020 provides the optical properties of particle ensembles composed of 20 irregular hexahedra, each ensemble uniquely characterized by the ratio of the particle total volume (V_i) to the total surface area A_i, expressed as the degree of sphericity Ψ_i. Lower Ψ_i values indicate more elongated particles as Ψ_i is inversely related to ε' of the corresponding regular hexahedral.

The mixtures of spheroids and irregular hexahedra are then constructed as follows: particle ensembles of spheroids are generated using random aspect-ratio distributions of 15 prolate and oblate shapes with aspect ratios ε' between 1.2 and 5.0, with mixing ratios f_i summing to 1. The prolate to oblate spheroid ratio also varies as p/o = 0.2, 0.5 and 0.8. Separate ensembles of irregular hexahedra are also constructed, each characterized by Ψ_i. Final mixtures are formed using random fractional contributions of spheroids (X_S) and irregular hexahedra (X_H), with $X_S + X_H$ =1.

The dust particle sizes are modelled using bimodal, log-normal size distributions derived from i) the corresponding AERONET products for ASKOS/JATAC campaign (see Section 3), and ii) the airborne in-situ measured size distributions, reported by [7]. The latter enables us to account for larger particle sizes, but also to provide a case of more generalized properties for transported dust.

For the real (n) and the imaginary (k) part of CRI, seventeen combinations are considered, considering dust climatological values [8], as well as airborne in-situ data from ASKOS.

Using different combinations of (i) shape mixtures, (ii) size distributions, and (iii) CRIs, we construct corresponding optical property look-up tables (LUTs). Then, the shape model that best reproduces the lidar observations of d_p and S_p, is derived by searching the LUTs for the value that minimizes the cost function in Eq. 1 (λ refers to wavelength, the superscripts M and S denote to the measurements and simulations respectively while e represents the measurement uncertainty).

$$\sum_{\lambda}\left(\left(\frac{d_{\lambda}^{M}-d_{\lambda}^{S}}{e(d_{\lambda}^{M})}\right)^{2}+\left(\frac{S_{\lambda}^{M}-S_{\lambda}^{S}}{e(S_{\lambda}^{M})}\right)^{2}\right)=min \qquad (1)$$

3. Example case study from the ASKOS/JATAC campaign

The JATAC/ASKOS ESA campaign was implemented in Cabo Verde during June and September 2022, mobilizing an extensive remote sensing measurement suite [9]. UAV flights equipped with optical particle counters (OPCs) and impactors were also performed to provide height-resolved, in-situ measurements of the particle size distribution and CRI. We select the day of June 26, 2022, as a case study to constrain the modelled optical properties with lidar observations. For this day, Fig. 2 shows the time-height plot of the volume linear depolarization ratio (d_v) at 532 nm, obtained by ground-based lidar.

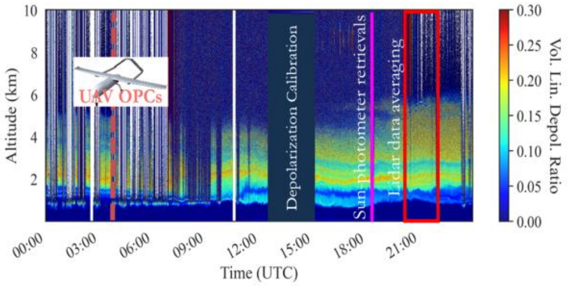

Figure 2. Time-height plot of d_v at 532 nm for the selected case study.

During the first half of the day, low-level clouds atop the marine boundary layer (MBL) strongly attenuate the lidar signal. The aerosol scene is otherwise homogeneous, with dust layers identified by elevated d_v values (0.2–0.25) extending from above the MBL up to 6 km, and evidence of dust mixing into the MBL (d_v up to 0.15 between 1 and 2 km height). The time window 20:45-21:30 UTC (red box) was selected to derive intensive dust properties at 355 and 532 nm. For 1064 nm, values of d_p are taken from airborne lidar data from NASA/CPEX campaign implemented in the same area; while S_p is taken from the literature (the low SNR on the particular day did not allow for a robust retrieval of this parameter). All values are summarized in Table 1.

Table 1. Lidar derived spectral d_p and S_p

λ [nm]	355	532	1064
Depolarization Ratio (d_p)			
ASKOS /CPEX	0.243 ± 0.024	0.3 ± 0.03	0.30-0.37
Lidar Ratio S_p [sr]			
ASKOS	58.5 ± 9	44.7 ± 7.4	58 ± 9 (*)

(*) Literature values [10]

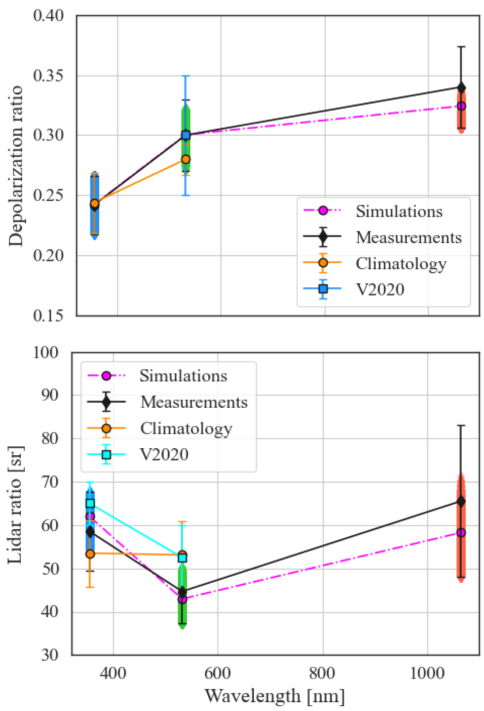

Figure 3. Comparison of d_p (up) and S_p (down) measurements, simulations and climatology

The reproduction of the lidar observations, using mixtures of spheroids and irregular-hexahedra, are shown in **Error! Reference source not found.**. The black lines indicate lidar observations of depolarization and lidar ratio. All calculated values in the LUTs that reproduce the lidar observations within their uncertainties are shown with different colored markers (blue, green and red for 355, 532 and 1064 nm respectively). The pink line indicates the LUT values that minimize the cost function. This result corresponds to i) a refractive index which indicates the origin of the particles to be the North Africa Sahara (imaginary part k: 0.0035, 0.0018 and 0.0008 at 0.355, 0.532 and 1.064 um respectively), largely consistent with the region of the measurements, ii) mainly prolate spheroids (p/o =0.8) and elongated hexahedra in the mixture (Ψ ~ 0.7). The orange and the light blue lines indicate climatology ranges and earlier studies [11 - 12], demonstrating that the new shape model reproduces the spectral dependence of d_p and S_p quite nicely and effectively captures the dust backscattering behavior. However, it has to be mentioned that these comparisons are only indicative, since a specific size distribution was used to derive the results presented herein.

4. Evaluation of the new shape model in reproducing multi-angular total and polarimetric radiances

To examine whether the derived shape model can reproduce angular measurements of total intensity, the same atmospheric scene from ASKOS (Fig. 2) is used, along with AERONET collocated observations. The dust layer is above 2 km, while below marine particle properties in high relative humidity (>90%) are found and considered in the simulations.

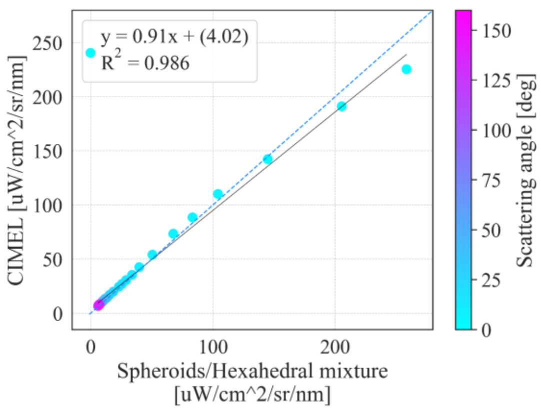

Figure 4. Comparison of simulated and AERONET measured radiances at 440 nm.

Figure 4 presents the comparison of simulated and measured radiances at 440 nm for an almucantar sun-photometer measurement geometry. Overall, there is a good agreement with $R^2 \approx 0.98$. The largest discrepancies of ~5%, are observed close to forward and side scattering angles (50–150°), which could likely be caused due to the assumed particle size distribution or assumed surface reflectance.

Similarly, the derived shape model is used to reproduce polarimetric data from the HARP2 instrument on board PACE for a selected scene over the Sahara outflow region. Figure 5 presents the PACE observations of the Degree of Linear Polarization (DoLP) and AOD at 670 nm, filtered for clouds; the pink line illustrates the footprint of ATLID lidar from the EarthCARE satellite overpass 1h after the PACE overpass. Profile of ATLID d_p is shown on the right for a random point across the lidar footprint (red dot) and reveals the dust plume below 6 km with typical mean d_p values around 20% at 355 nm.

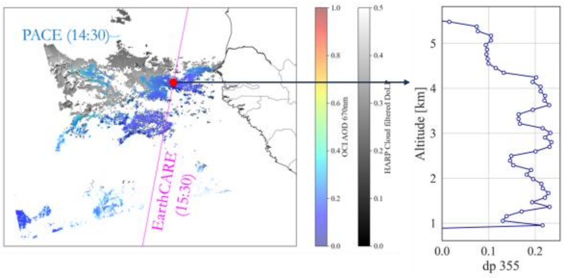

Figure 5. (left) HARP2 DoLP (grey colors), and PACE/OCI AOD values (blue colors) at 670 nm and (right) ATLID d_p profile at 355 nm.

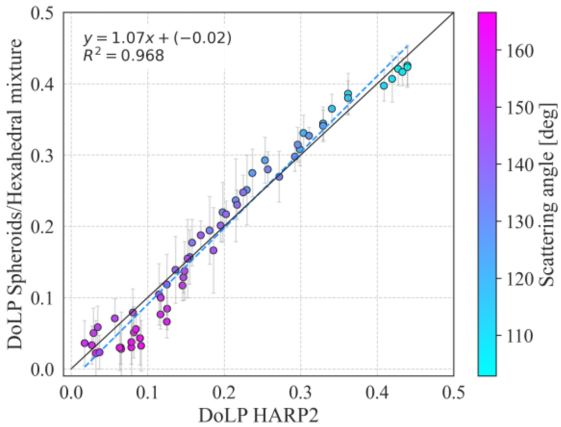

Figure 6. Comparison of simulated and HARP2 measured radiances at 670 nm.

A preliminary comparison of the simulated against measured DoLP at 670 nm is shown in Fig. 6 for the random point shown on Fig. 5. Overall ,there is a good agreement for this first comparison with simulation results within the measurements uncertainties and $R^2 \approx 0.97$. Further work is on-going to reproduce the DoLP for this whole atmospheric scene.

5. Conclusions and future work

Herein, we provide updated optical properties for non-spherical dust particles assuming random shape mixtures of spheroids and irregular hexahedra, which successfully reproduce spectral lidar observations. Preliminary results indicate that this new shape model for dust may also be used to reproduce passive remote sensing observations. The new shape model is being applied in data assimilation studies using EarthCARE and PACE observations, as well as in radiative closure simulations with airborne and EarthCARE measurements [13]. These efforts aim to exploit the full potential of advanced remote-sensing data and demonstrate the added value for atmospheric composition modelling, as well as to contribute to improved estimates of dust radiative forcing and heating rates.

References

[1] Kok et al., *Nature Geoscience, 10(4), 274–278* (2017)

[2] Dubovik et al., *Journal of Geoph. Res., 111(D11), D11208* (2006)

[3] Saito et al., *Journal of the Atm. Sci., 78(7), 2089–2111* (2021)

[4] Gasteiger at al., *Tellus B: Chem. and Phys. Meteor., 63(4), 725–741* (2011)

[5] Varga et al., *Sedimentary Geology*, 370, 1–14 (2018)

[6] Gasteiger and Wiegner, *Geosci. Model Dev., 11, 2739–2762* (2018)

[7] Ryder et al., *Atmos. Chem. Phys., 18, 17225–17257* (2018)

[8] Di Biagio et al., *Atmos. Chem. Phys.*, 19, 15503–15531 (2019)

[9] Marinou et al., *Environmental Sciences Proceedings, 26(1)* (2023)

[10] Haarig et al., *Atmos. Chem. Phys., 22, 355–369 (2022)*

[11] Floutsi et al, *Atmos. Meas. Tech., 16, 2353–2379* (2023)

[12] Veselovsii et al, *Atmos. Chem. Phys., 16, 7013–7028* (2016)

[13] Kouklaki et al., *EGU General Assembly, EGU25-1057* (2025)

Acknowledgements:

This research has been financially supported by the CERTAINTY Horizon Europe project (GA No 101137680), the AIRSENSE ESA project (Contr. No. 4000142902/23/I-NS) and the EarthCARE - DISC ESA project (Contr. No. 4000144997/24/I-NS. It is also based upon work performed within EARLICOST, CA24135, supported by COST (European Cooperation in Science and Technology).